Металлофиз. новейшие технол. / Metallofiz. Noveishie Tekhnol.
2016, т. 38, № 10, сс. 1279–1292 / DOI: 10.15407/mfint.38.10.1279
Оттиски доступны непосредственно от издателя
Фотокопирование разрешено только
в соответствии с лицензией

© 2016 ИМФ (Институт металлофизики
им. Г. В. Курдюмова НАН Украины)

Напечатано в Украине.

ДЕФЕКТЫ КРИСТАЛЛИЧЕСКОЙ РЕШЁТКИ

PACS numbers: 61.72.Bb, 61.72.jd, 61.72.Qq, 64.75.Op, 66.30.Ny, 68.35.Dv, 68.35.Fx

Competition of Voiding and Kirkendall Shift during Compound Growth in Reactive Diffusion—Alternative Models

T. V. Zaporozhets, N. V. Storozhuk, and A. M. Gusak

Bohdan Khmelnytsky National University of Cherkasy,
81 Shevchenko Blvd.,
18031 Cherkasy, Ukraine

The simultaneous growth of both the phase-layer thickness and the void sizes during the intermetallic-compound formation with different mobilities of components and with a narrow concentration-range of homogeneity is described. This is done with account of competition for extra vacancies between dislocation steps and interfaces (K-sinks leading to Kirkendall shift) and voids (F-sinks providing Frenkel voiding). Three alternative models for three alternative places of preferential voids' formation are formulated and compared. Possibilities of control over Kirkendall shift versus Frenkel voiding competition are discussed.

Key words: diffusion, reaction, phase-growth law, voids, intermetallic compounds.

Описано одночасний ріст товщини прошарку фази та розмірів пор у процесі формування інтерметалевої сполуки у системі з відмінними рухливостями компонентів і з вузьким концентраційним інтервалом гомогенности. При цьому враховано конкуренцію зайвих вакансій між дислокаційними сходинками та міжфазними інтерфейсами (K-стоками, які приводять до Кіркендаллового зміщення) і порами (F-стоками, які забезпечують Френкелеве пороутворення). Запропоновано і порівняно три альтернативні моделі для трьох альтернативних місць переважного зародження пор. Обговорюються можливості контролю конкуренції Кіркендаллового зміщення і Френкелевого пороутворення.

Corresponding author: Tetyana Vasylivna Zaporozhets
E-mail: zaptet@ukr.net

Please cite this article as: T. V. Zaporozhets, N. V. Storozhuk, and A. M. Gusak, Competition of Voiding and Kirkendall Shift during Compound Growth in Reactive Diffusion—Alternative Models, *Metallofiz. Noveishie Tekhnol.*, **38**, No. 10: 1279–1292 (2016), DOI: 10.15407/mfint.38.10.1279.

Ключові слова: дифузія, реакції, закон росту фази, пори, інтерметалева сполука.

Описан одновременный рост толщины слоя фазы и размеров пор в процессе формирования интерметаллического соединения в системе с различными подвижностями компонентов и с узким концентрационным интервалом гомогенности. При этом учтена конкуренция избыточных вакансий между дислокационными ступеньками и межфазными интерфейсами (*K*-стоками, которые приводят к киркендалловскому смещению) и порами (*F*-стоками, обеспечивающими порообразование по Френкелю). Проведён сравнительный анализ трёх альтернативных моделей для трёх альтернативных мест преимущественного зарождения пор. Обсуждаются возможности контроля конкуренции киркендалловского смещения и порообразования по Френкелю.

Ключевые слова: диффузия, реакции, закон роста фазы, поры, интерметаллические соединения.

(Received July 29, 2016)

1. INTRODUCTION

Reactive diffusion (growth of single or several intermediate phase layers in the contact zone of two materials) is often accompanied by voiding—formation and growth of voids inside these layers or at their interfaces or in the neighbouring material. Sometimes, this phenomenon can be useful—as for fabrication of hollow nanoshells for drug delivery and other applications [1–5]. Yet, typically, voiding is harmful and eventually leads to failures of joints under repeating loadings and stresses. For example, in soldering, the reaction of copper with tin-based solder leads to formation of two intermetallic phases Cu_6Sn_5 and Cu_3Sn [6]. In particular, the growth of the latter (Cu_3Sn), typically, leads to formation and growth of multiple voids. Voids formation, in principle, can be related to molar volume changes during phase transformations. Yet, voiding during Cu_3Sn growth is usually called the Kirkendall voiding. It proceeds because diffusivity of copper inside the growing Cu_3Sn phase is much larger than that of tin [7]. It leads to large vacancy flux inside the growing Cu_3Sn phase layer, directed from tin to copper. Hence, supersaturation with vacancies is formed in the vicinity of interface $Cu_3Sn|Cu$.

The relaxation of vacancy supersaturation can proceed *via* at least two ways. The first way is voiding because of vacancy relaxation at the so-called *F*-sinks (terminology of Ya. E. Geguzin [8]), which means just joining of vacancies into voids (pores). The second way is vacancy relaxation without voiding, at the so-called *K*-sinks, according to the same terminology of Ya. E. Geguzin (at dislocation kinks or at the grain boundaries, leading eventually to Kirkendall shift). The compe-

tition of the *K*- and *F*-sinks during interdiffusion was studied by Geguzin's group in experiments with diffusion couples at relatively low pressures [8, 9]. In particular, the pressure of up to 100 atm was shown to almost completely suppress the void formation, although it almost did not change the frequencies of diffusion jumps. Thus, the Frenkel effect practically vanished during interdiffusion, whereas the Kirkendall effect (marker shift due to lattice shift) became stronger.

Intuitively, pressure is not a unique method of voiding suppression. One can also try to increase a density of the *K*-sinks (say, dislocation density) or/and decrease a density of heterogeneous void nucleation sites. Main equations describing the competition of the *K*- and *F*-sinks were published in [10] for homogeneous alloys as well as for inter- and reactive diffusion [11]. As we now can see, the models presented in [10, 11], were too limited. Here, we will develop three alternative models of *K*-sinks versus *F*-sinks competition in reactive diffusion. These three models differ by the place of void nucleation and, hence, by the mechanism of growth.

In the intermediate phase Cu_3Sn of the binary couple Cu|Sn, the main diffusant is copper ($D^*_{Sn} << D^*_{Cu}$). Diffusion of copper through the phase layer generates the inverse vacancy flux directed from tin (or from neighbouring phase Cu_6Sn_5) to copper. This vacancy flux is essentially stopped somewhere in the vicinity of interface Cu_3Sn|Cu (IMC|B). If extra vacancies are consumed by the *K*-sinks, it gives just the Kirkendall shift—phase layer moves as a whole towards copper filling the emptiness generated by outgoing vacancy flux. Yet, if, by some reasons, the *K*-sinks are not powerful enough, voids nucleate and grow. At that, we consider three cases. CASE 1: Voids can appear inside the phase layer, closer to interface Cu_3Sn|Cu (narrow IMC-layer in M1 in Fig. 1). This version correlates with the fact that the intermedi-

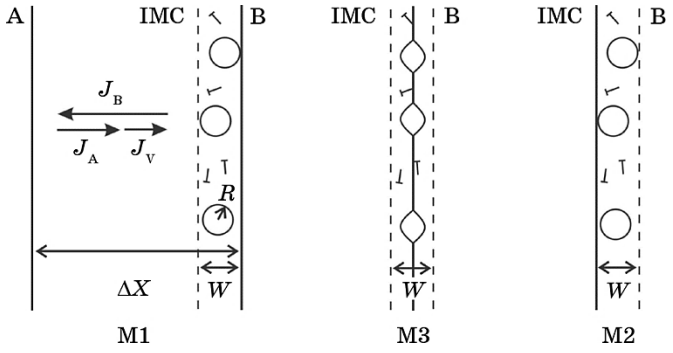

Fig. 1. Three models of possible voids' formation due to vacancy supersaturation in the vicinity of interface IMC|B—in some zone (of width *W*) of effective vacancy sinks: M1—inside IMC, M3—directly at the interface IMC|B, M2—in pure B.

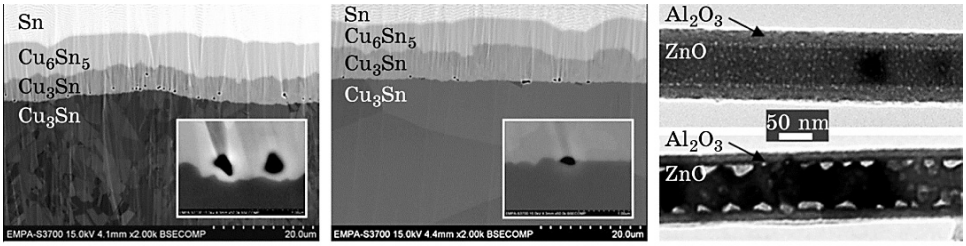

a *b* *c*

Fig. 2. Morphology of reaction zone with different void location: SEM image of diffusion couple 'electroplated Cu|liquid Sn', after 188 hours of annealing at 210°C (inserted—96 hours) (*a*); SEM image of diffusion couple 'Cu after recrystallization annealing|liquid Sn', after 188 hours of annealing at 210°C (inserted—96 hours) (*b*); TEM image of cylindrical core-shell system ZnO|Al_2O_3 after 15 hours at 600°C [3] (*c*).

ate phase contains 25 percent of the low-melting tin, so that vacancy formation and migration energies are lower than those in copper are. Indeed, in the SEM images, many voids can be noticed inside the phase layer (Fig. 2, *a*). On the other hand, many voids can be seen directly at the interface Cu_3Sn|Cu. It gives us CASE 3—model M3 in Fig. 1. This case of heterogeneous nucleation looks like more probable (Fig. 2, *b*), especially at the joints of interface with grain boundaries in the growing phase or in copper. CASE 2 (nucleation at the copper side) is also possible since the vacancy flux compensates the flux of copper from copper side—model M2 in Fig. 1. CASE 2 is realized in the formation of hollow nanoshells and was described qualitatively by Goesele *et al.* in the bridge model [3] and mathematically (for the case of one surviving central void) in [4, 5] (Fig. 2, *c*).

One can find experimental evidence for each of three possible voids locations [12, 13]. Yet, the location of the void inside the growing phase layer does not guarantee that this void nucleated within this layer (alternatively, it can be incorporated into the growing phase from the parent phase). During phase layer growth, the void can (a) migrate in the concentration gradient, (b) move together with surrounding lattice, (c) move together with (be pinned and dragged by) moving interface. Therefore, classification of cases is directly related only to initial stages of the void.

Below, we present the phenomenological models of void formation for the abovementioned three cases (structures).

2. MODELS

We treat voiding as a result of heterogeneous nucleation at some suita-

ble sites. To simplify the analysis, we consider a net of the K- and F-sinks. We treat all F-sinks as the same in one cross-section (so far we do not take into account the size distribution and ripening of voids). K-sinks are the steps and kinks at interfaces and dislocations. Their effectiveness is characterized by the mean free path length L_V or means relaxation time τ_V ($L_V^2 \sim D_V\tau_V$). Concrete meaning of L_V in models M1, M2 and M3 may be different: for models M1 and M2, the value of L_V, most probably, is determined by the dislocations density in the bulk of the IMC or in pure B, for model M3 the L_V is determined by the morphology of interface.

Let us consider the growth of IMC with mean stoichiometric composition c_B^{IMC} and narrow homogeneity range Δc_B^{IMC}. If the tracer diffusivities D_A^*, D_B^* significantly differ, $D_A^* \ll D_B^*$, then the vacancy flux is significant and directed from A to B (as shown for M1 in Fig. 1).

Basic equations. Growth kinetics of the intermediate phase layer of width ΔX because of reaction between two almost pure materials with small mutual solubilities is described by the equation [8]:

$$\frac{d\Delta X}{dt} = -\frac{1}{c_B^{IMC}(1-c_B^{IMC})}\Omega J_B. \qquad (1)$$

Here, Ω is an average atomic volume, the flux density J_B is determined in the laboratory reference frame, it is almost the same in all sections ($\partial\Omega J_B/\partial x \approx 0$), but of course, decreases with time due to a decrease of mean average concentration gradient. It means a steady-state approximation. This approximation works the better—the less is the concentration range of IMC [14, 15].

In general case, when system is still characterized by the nonequilibrium vacancy redistribution, the flux density in the laboratory reference frame contains two terms—first term proportional to the concentration gradient ∇c_B (or chemical potential gradient $\nabla\mu_B$) of one of the basic components, second term—proportional to the vacancy concentration gradient ∇c_V (or vacancy chemical potential gradient $\nabla\mu_V = \nabla(kT\ln(c_V/c_V^{eq}))$:

$$\Omega J_B = -D_D\nabla c_B - (1-c_B^{IMC})c_B^{IMC}\frac{(D_B^*-D_A^*)}{kT}\nabla\mu_V. \qquad (2)$$

Here, $D_D = ((1-c_B^{IMC})D_B^* + c_B^{IMC}D_A^*)\varphi$ —Darken interdiffusivity with the thermodynamic factor $\varphi = \frac{c_B}{kT}\frac{\partial\mu_B}{\partial c_B} = \frac{c_A c_B}{kT}\frac{\partial^2 g}{\partial c_B^2}$. Vacancy chemical potential $\mu_V = kT\ln(c_V/c_V^{eq})$ becomes zero when vacancy concentration reaches an equilibrium value c_V^{eq}.

In most cases, the components of diffusion couple have different

melting points. Therefore, the properties of compound interfaces with two parent phases differ significantly. The interface between the compound and low-melting component, most probably, does not cause any delay with supply of vacancies and crossing of interface barriers by the migrating atoms. Respectively, in our model, we will treat vacancies at the left interface A|IMC to be always in equilibrium and their chemical potential to be zero. The main deviation of vacancies from equilibrium is expected in the vicinity of interface IMC|B. As mentioned above, here one can distinguish three versions of vacancy sinks working in the vicinity of this interface.

Let W be the width of the vacancy sinks zone (to be specified in each case) and S—the cross-section area. Then, the total vacancy number $N_V = c_V^W WS/\Omega$ in the sinks zone changes according to the following the balance equation:

$$SW \frac{d(c_V^W)}{dt} = j_V S - 0 - \frac{dN_V^K}{dt} - \frac{dN_V^F}{dt}. \tag{3}$$

In equation (3), zero in the right-hand side demonstrates that the vacancy flux enters the sinks zone but does not leave it. All incoming vacancies go to K- or, alternatively, to F-sinks. In case of small deviation from equilibrium, the action of K-sinks is traditionally described in the frame of relaxation approximation:

$$\frac{dN_V^K}{dt} \cong N_V \frac{c_V(t) - c_V^{eq}}{\tau_V} dt. \tag{4}$$

At the initial stages of reactive diffusion, the vacancy supersaturation may be significant. In this case, it seems reasonable to use the difference of chemical potentials (instead of deviation of vacancy concentration) as a true driving force of vacancy relaxation. Let us make some 'inverse simplification':

$$\frac{c_V(t) - c_V^{eq}}{\tau_V} = D_V c_V^{eq} \frac{c_V(t)/c_V^{eq} - 1}{D_V \tau_V} \approx D_V c_V^{eq} \frac{\ln(c_V(t)/c_V^{eq})}{L_V^2} = \frac{D_V c_V^{eq} \mu_V}{L_V^2 kT}.$$

Then,

$$\frac{dN_V^K}{dt} \cong \frac{WS}{\Omega} \frac{D_V^W c_V^{eq}}{L_V^2} \frac{\mu_V^W}{kT}. \tag{5}$$

One can expect that equation (5) is more general and is reduced to equation (4) at small deviations from equilibrium.

Rate of vacancy elimination at growing voids is proportional to the number of void heterogeneous nucleation sites per unit interface area n_s:

$$\frac{dN_{\mathrm{V}}^{\mathrm{F}}}{dt} \cong \frac{n_{\mathrm{s}} S}{\Omega} \frac{dV_{\mathrm{void}}}{dt}. \tag{6}$$

Here, dV_{void} / dt —void volume growth rate (void being treated as a sphere with radius r in models M1 and M2 or lens-type with cross-section of radius r along interface in model M3).

The void growth rate is affected by the action of K-sinks around the void. This problem was considered recently in [8]. Modifying result of [8] in terms of vacancy chemical potential, one can write:

$$\frac{dr}{dt} = ((1 - c_{\mathrm{B}}^{\mathrm{IMC}}) D_{\mathrm{A}}^{*} + c_{\mathrm{B}}^{\mathrm{IMC}} D_{\mathrm{B}}^{*}) \frac{\mu_{\mathrm{V}}^{W}}{kT} \left(\frac{1}{r} + \frac{1}{L_{\mathrm{V}}} \right). \tag{7}$$

Gradient of vacancy chemical potential is included in the vacancy flux:

$$\Omega j_{\mathrm{V}} = (D_{\mathrm{B}}^{*} - D_{\mathrm{A}}^{*}) \varphi \frac{\Delta c}{\Delta X} - \frac{D^{W}}{\Delta X} \frac{\mu_{\mathrm{V}}^{W}}{kT}. \tag{8}$$

This expression can be used on the right-hand side of equation (3). The left-hand side of equation (3) can be treated as zero, in the frame of steady-state approximation for vacancies. This approximation is the result of vacancy high mobility. Thus, after substitution of equations (5), (6), (8) into equation (3) with zero in the left-hand side one obtains an equation for determination of the unknown $\mu_{\mathrm{V}}^{W} / kT$.

Evaluation of effective sinks zone width W. The width of the vacancy sinks zone depends on the nature of sinks. For the model M3, it is reasonable to consider both K- and F-sinks located at the interface. Therefore, in this model, we take $W \sim \delta$, where δ is an interface width (about nanometre).

In the case of models M1, M2, the sinks are present, theoretically, all over the phase layer. Yet, as we already discussed before equation (3), essential deviation of vacancies from equilibrium is expected only in the vicinity of interface IMC|B. Let us find the vacancy chemical potential along the phase layer. For this, we use the steady-state approximation not only for vacancies but as well for base components:

$$\begin{cases} \dfrac{\partial c_{\mathrm{B}}}{\partial t} = -\dfrac{\partial}{\partial x} (\Omega J_{\mathrm{B}}) \approx 0, \\ \dfrac{\partial c_{\mathrm{V}}}{\partial t} = -\dfrac{\partial}{\partial x} (\Omega j_{\mathrm{V}}) - \dfrac{c_{\mathrm{V}}^{\mathrm{eq}}}{\tau_{\mathrm{V}}} \dfrac{\mu_{\mathrm{V}}(x)}{kT} \approx 0. \end{cases} \tag{9}$$

(Correctness of steady-state approximation for compounds with narrow homogeneity range was first proved in [15].) In the second equation (9), the relaxation of vacancies at K-sinks is taken into account.

Substitution of equation (8) into second equation (9) leads to equation:

$$\left(\frac{\partial^2}{\partial x^2} - \frac{1}{D_V \tau_V}\right)\frac{\mu_V(x)}{kT} \approx \frac{(D_B^* - D_A^*)\varphi}{c_V^{eq} D_V}\frac{\partial^2 c_B}{\partial x^2}. \quad (10)$$

The first equation (9) means that the flux of the main component within the phase layer is almost constant along x. Then, using equation (2) for this flux, one can express $\partial^2 c_B/\partial x^2$ in terms of vacancy chemical potential:

$$\frac{\partial^2 c_B}{\partial x^2} \approx \frac{c_B^{IMC}(1 - c_B^{IMC})(D_B^* - D_A^*)\varphi}{D_D}\frac{\partial^2}{\partial x^2}\left(\frac{\mu_V(x)}{kT}\right). \quad (11)$$

The combination of equations (10), (11) gives the resulting equation for vacancy chemical potential:

$$\frac{D_{NG}}{D_D}\frac{\partial^2}{\partial x^2}\left(\frac{\mu_V(x)}{kT}\right) \approx \frac{1}{L_V^2}\frac{\mu_V(x)}{kT}. \quad (12)$$

Here, $D_{NG} = D_A^* D_B^* \varphi / (c_B^{IMC} D_B^* + (1 - c_B^{IMC}) D_A^*)$ is a Nazarov–Gurov (Nernst–Planck) diffusion coefficient [16, 14].

Equation (12) is a typical screening equation with screening length $L_V\sqrt{D_{NG}/D_D}$, which can be treated as effective vacancy mean free path L_V^{ef} with account of the inverse Kirkendall effect: the local flux of vacancies to sink generates local segregation due to the difference of components mobilities, segregation effect influences the vacancy flux and makes this flux less. Note that the ratio D_{NG}/D_D tends to zero when one of the components is much faster than another one, and in this case, the effective mean free path becomes significantly less. At equal mobilities of the components, the L_V^{ef} tends to L_V. Thus, the width W of effective sinks zone should be taken as L_V^{ef} in the model M1, L_V in the model M2. In short, $W_{M1} = L_V^{ef}$, $W_{M2} = L_V$, $W_{M3} = \delta$.

Kinetics of intermediate phase growth and void growth. We use equations (3), (5), (6), (8) for determination of vacancy chemical potential, equation (1)—for determination of phase width, equation (7)—for determination of void radius. At that, in each model, we use the corresponding diffusivity D^W (D^{IMC}, D^B, D^{int} respectively for the models M1, M2, M3). We omit the long algebra and give only final expression after the transition to dimensionless variables.

In the case of models M1, M2, we used dimensionless parameter $Q = \delta/(n_s 4\pi L_V^3)$, dimensionless phase width $\xi = \Delta X/X^*$, void radius $\rho = R/R^*$ and time $\tau = tD_D\Delta c/(\Delta X^*)^2$, where characteristic sizes are as

follow: $\Delta X^* = L_V^2 / \delta$, characteristic phase width corresponding to crossover from linear to parabolic phase growth kinetics [17],

$$R^* = \delta / (n_s 4\pi L_V^2) = (4\pi n_s \Delta X^*)^{-1} \propto Y^2 / \Delta X^*$$

(Y is an average lateral distance between voids), $Q = R^*/L_V$.

As a result, for the model M1, we get the expressions for $\mu_V^W/(kT)$, for phase growth rate $d\xi/d\tau$ and for void growth rate $d\rho/d\tau$:

$$\frac{\mu_V^W}{kT} = \frac{(D_B^* - D_A^*)\varphi\Delta c}{D^{IMC}} \frac{1}{1 + \xi(1 + \rho(1 + Q\rho))}, \tag{13}$$

$$\frac{d\xi}{d\tau} = \frac{1}{c_B^{IMC}(1 - c_B^{IMC})} \frac{\dfrac{D^{NG}}{D^D} + \xi(1 + \rho(1 + Q\rho))}{1 + \xi(1 + \rho(1 + Q\rho))} \frac{1}{\xi}, \tag{14}$$

$$\frac{d\rho}{d\tau} = \frac{(D_B^* - D_A^*)}{D^D} \varphi\left(\frac{4\pi n_s L_V^4}{\delta^2}\right)^2 \frac{(1 + Q\rho)}{1 + \xi(1 + \rho(1 + Q\rho))} \frac{1}{\rho}. \tag{15}$$

For the model M2, one gets:

$$\frac{\mu_V^W}{kT} = \frac{(D_B^* - D_A^*)\varphi\Delta c}{D^{IMC}} \frac{1}{1 + \dfrac{D^B}{D^{IMC}} \xi(1 + \rho(1 + Q\rho))}, \tag{16}$$

$$\frac{d\xi}{d\tau} = \frac{1}{c_B^{IMC}(1 - c_B^{IMC})} \left(\frac{\delta}{L_V}\right)^2 \frac{\dfrac{D^{NG}}{D^D} + \dfrac{D^B}{D^{IMC}} \xi(1 + \rho(1 + Q\rho))}{1 + \dfrac{D^B}{D^{IMC}} \xi(1 + \rho(1 + Q\rho))} \frac{1}{\xi}, \tag{17}$$

$$\frac{d\rho}{d\tau} = \frac{(D_B^* - D_A^*)}{D^D} \frac{D^B}{D^{IMC}} \varphi\left(\frac{1}{Q}\right)^2 \frac{(1 + Q\rho)}{1 + \dfrac{D^B}{D^{IMC}} \xi(1 + \rho(1 + Q\rho))} \frac{1}{\rho}. \tag{18}$$

In the case of model M3, mainly equation (7) is changed—we consider the $2D$ supply of vacancies along $2D$ interface for the construction of $3D$ (lens-type) void. Simple but long algebra with introduction of non-dimensional parameter $P = (L_V/R^{max})^2$, where $R^{max} = (n_s\pi)^{-1/2}$ (about this threshold voids will fill the total cross-section), $\rho = R/R^{max}$ gives:

$$\frac{\mu_V^W}{kT} = \frac{(D_B^* - D_A^*)\varphi\Delta c}{D^{IMC}} \frac{1}{1 + \dfrac{D^{int}}{D^{IMC}} \xi\left(1 + \dfrac{2P}{(1 - \rho^2)\ln(1/\rho)}\right)}, \tag{19}$$

$$\frac{d\xi}{d\tau} = \frac{1}{c_{\mathrm{B}}^{\mathrm{IMC}}(1-c_{\mathrm{B}}^{\mathrm{IMC}})} \frac{\dfrac{D^{\mathrm{NG}}}{D^{\mathrm{D}}} + \dfrac{D^{\mathrm{int}}}{D^{\mathrm{IMC}}}\xi\left(1+\dfrac{2P}{(1-\rho^2)\ln(1/\rho)}\right)}{1+\dfrac{D^{int}}{D^{IMC}}\xi\left(1+\dfrac{2P}{(1-\rho^2)\ln(1/\rho)}\right)} \frac{1}{\xi}, \tag{20}$$

$$\frac{d\rho}{d\tau} = \frac{\pi}{\Psi}\frac{(D_{\mathrm{B}}^{*}-D_{\mathrm{A}}^{*})}{D^{\mathrm{D}}}\frac{D^{\mathrm{int}}}{D^{\mathrm{IMC}}}\frac{PL_{\mathrm{V}}^{2}}{\pi n_{\mathrm{s}}\delta} \frac{\left(\dfrac{2}{\ln(1/\rho)}+\left(\dfrac{\rho}{P}\right)^{2}\left(1+\dfrac{2P}{(1-\rho^2)\ln(1/\rho)}\right)\right)}{1+\dfrac{D^{\mathrm{int}}}{D^{\mathrm{IMC}}}\xi\left(1+\dfrac{2P}{(1-\rho^2)\ln(1/\rho)}\right)} \frac{1}{\rho^2}, \tag{21}$$

where

$$\Psi = \frac{4\pi}{\sin^3\Theta}\left(\frac{2}{3}-\cos\Theta+\frac{1}{3}\cos^3\Theta\right). \tag{22}$$

3. ANALYSIS

Below, we suggest some numerical and asymptotic analysis to assess the feasibility of the proposed models.

First, we solve numerically equations (13)–(21) with the calculation of annihilation at the *K*- and *F*-sinks, $N_{\mathrm{V}}^{\mathrm{K}}$, $N_{\mathrm{V}}^{\mathrm{F}}$, according to equations (5), (6). An example of numeric calculation in the case of M1 is demonstrated in Fig. 3. Calculations were made for various values of mean free path of vacancies L_{V} at fixed density of void nucleation sites n_{s} (Fig. 3, *a*). Alternatively, calculations were made for various densities n_{s} of void nucleation sites at fixed L_{V} (Fig. 3, *b*). Evidently, the growth laws for compound layer thickness ΔX and for average void radius R are no universal for different stages. Therefore, at the right of Fig. 3, we demonstrate the exponents of power dependencies $\xi \approx k\tau^m$, $m = d\ln\xi/d\ln\tau$ and $\rho \approx \beta\tau^q$, $q = d\ln\rho/d\ln\tau$.

Second, asymptotic behaviour at various stages is studied. For example, for model M1, we can distinguish some asymptotic regimes. At $D_{\mathrm{NG}}/D_{\mathrm{D}} \ll 1$ and $\rho \ll 1$, the following subregimes with different power laws $\xi \approx k\tau^m$, $\rho \approx \beta\tau^q$ can be found (see Table 1).

In general, asymptotic analysis of model M1 gives 6 principal regimes, differing with time exponents of the dependencies $m = d\ln\xi/d\ln\tau$, $q = d\ln\rho/d\ln\tau$ at $m = 1/2$, 1, 3/2, 2 and $q = 1/2$, 1/4, 1/6 (Fig. 4).

Regimes I, II, III correspond to phase growth with an account of vacancies redistribution but practically without feedback from voiding. In Regime I, the parabolic growth of phase layer is controlled by the slower diffusant (*via* Nernst–Planck, or Nazarov–Gurov, combination of diffusivities, $D_{\mathrm{NP}} = D_{\mathrm{NG}} = D_{\mathrm{A}}D_{\mathrm{B}}/(c_{\mathrm{A}}D_{\mathrm{A}} + c_{\mathrm{B}}D_{\mathrm{B}})$ [14]). The growth of

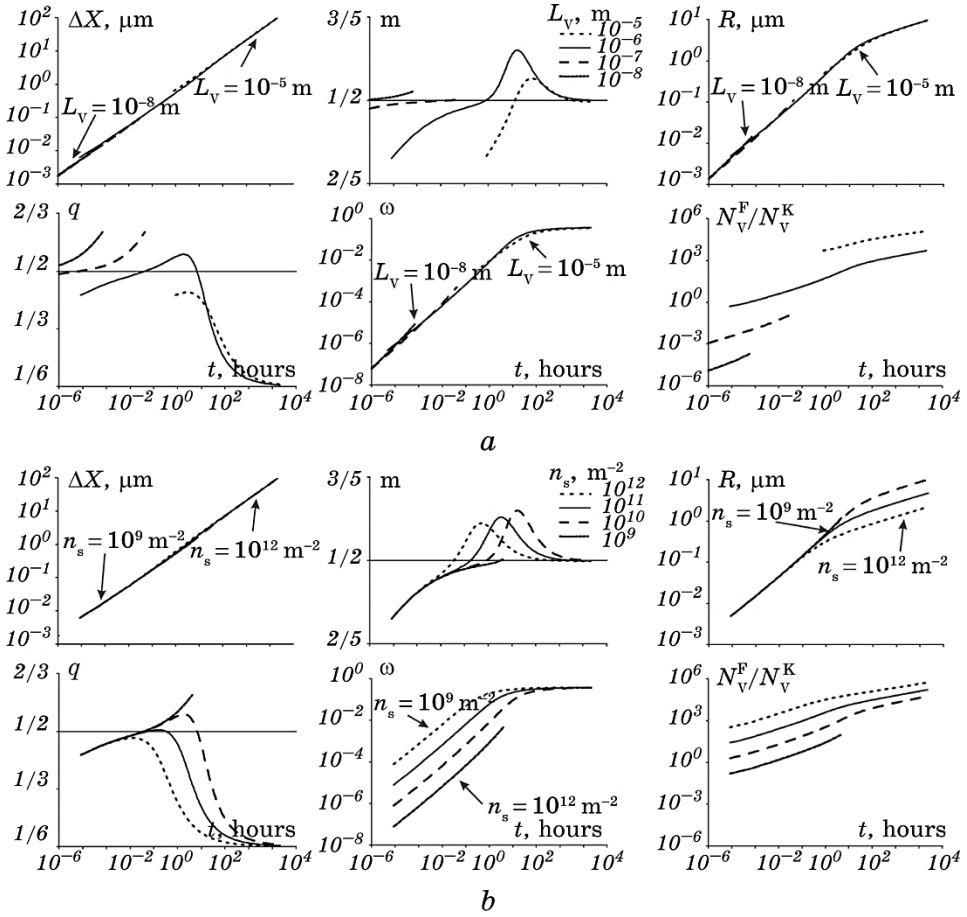

Fig. 3. Example of numeric calculations for the case of model M1 (regime IV at Fig. 4) at $n_s = 10^{10}$ m^{-2}, $L_V = 10^{-8}$–10^{-5} m (*a*) and $L_V = 1$ μm, $n_s = 10^9$–10^{12} m^{-2} (*b*). The parameter ω—void fraction (ratio of the total voids volume to the phase layer volume).

voids is also parabolic and is controlled by the difference of diffusivities. Regime II is a transient one (with linear phase growth) to another parabolic regime but controlled by the faster component (*via* Darken combination of diffusivities, $D_D = c_B D_A + c_A D_B$). In Regimes III and IV, the phase layer growth kinetics remains parabolic but the void growth kinetics is changed. Regimes V and VI are most exotic but have not too many chances of realization in the real systems (large voids in the thin phase layer are difficult to imagine).

In the case of model M2, the regimes and time exponents, similar to the case of model M1, can be obtained at the intervals $\xi D^B/D^{IMC} << D_{NG}/D_D$, $D_{NG}/D_D << \xi D^B/D^{IMC} << 1$, $\xi D^B/D^{IMC} >> 1$, along axis ξ

TABLE 1.

	$\xi << D_{NG}/D_D$	$D_{NG}/D_D << \xi << 1$	$1 << \xi$
$d\xi/d\tau$	$\frac{1}{c_B^i(1-c_B^i)}\frac{D_{NG}}{D_D}\frac{1}{\xi}$	$\frac{1}{c_B^i(1-c_B^i)}\frac{1}{2}$	$\frac{1}{c_B^i(1-c_B^i)}\frac{1}{\xi}$
ξ	$\sqrt{\frac{2}{c_B^i(1-c_B^i)}\frac{D_{NG}}{D_D}}\sqrt{\tau}$	$\frac{1}{2c_B^i(1-c_B^i)}\tau$	$\sqrt{\frac{2}{c_B^i(1-c_B^i)}}\sqrt{\tau}$
m	1/2	1	1/2
ρ	$\sqrt{\frac{2(D_B^*-D_A^*)\varphi}{D_D}}\frac{R^*}{\delta}\sqrt{\tau}$	$\sqrt{\frac{2(D_B^*-D_A^*)\varphi}{D_D}}\frac{R^*}{\delta}\sqrt{\tau}$	$\sqrt{\frac{2(D_B^*-D_A^*)\varphi}{D_D}\sqrt{2c_B^i(1-c_B^i)}}\frac{R^*}{\delta}\tau^{1/4}$
q	1/2	1/2	1/4

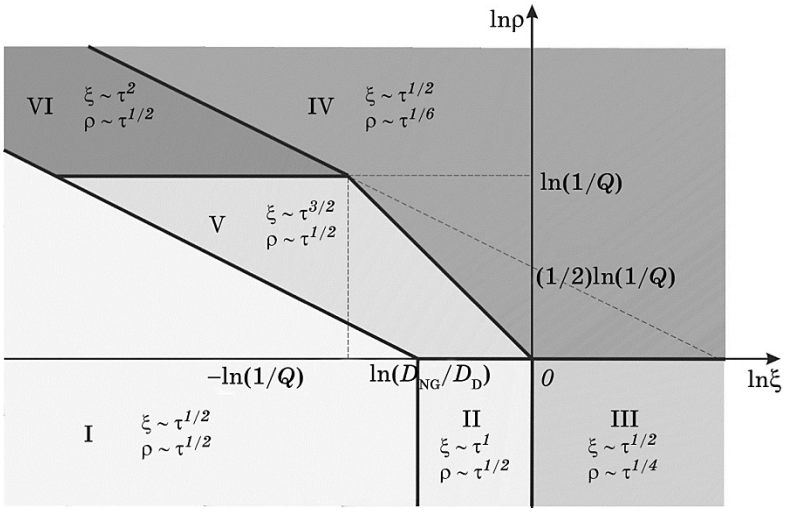

Fig. 4. Map of asymptotic regimes for model M1.

and intervals $\rho << 1$, $1 << \rho << 1/Q$, $\rho >> 1/Q$ along the axis ρ.

One can see that at various stages of reactive growth the time exponents of layer growth and especially of void growth may change rather significantly. Thus, the experimental systematic study of voiding in various regimes looks promising. Of course, one should remember about natural constraints for void growth (like $\pi R^2 n_s < 1$).

4. SUMMARY

Three alternative models of void formation during reactive growth of

compound layer were suggested taking into account Kirkendall-type vacancies' sinks (dislocations, grain boundaries) as well as Frenkel-type vacancies' sinks (voids). For each case, the self-consistent set of equations compound growth and void growth kinetics are formulated and partially analysed. To choose the right model for given system, additional experiments are needed. The vacancy mean free migration path length L_V appears to be especially important for void growth and, in principle, can be used as one of the parameters controlling the voiding kinetics. Another major parameter is a density of heterogeneous void nucleation sites. If one provides more effective work of K-sinks, one can expect less voiding (less activity of F-sinks). Providing more effective work of K-sinks can be realized by increasing of dislocation density, if this effect will not be eliminated by recrystallization. For this, one needs to anneal at sufficiently low temperature.

This research was supported by a Marie Curie International Research Staff Exchange Scheme Fellowship within the 7th European Community Framework Programme (Ref. 612552) and by Ministry of Education and Science of Ukraine (project 0115U000638 and 0116U004691). Authors are grateful to Csaba Cserhati and Zoltan Erdélyi (University of Debrecen, Hungary) for fruitful discussions, to Oleksii Liashenko (University of Grenoble) for sharing experimental evidence, and also to Lab for Joining Technologies and Corrosion (EMPA, Switzerland) for the opportunity of SEM study.

REFERENCES

1. Y. Yin, R. M. Rioux, C. K. Erdonmez, S. Hughes, G. A. Somorjai, and A. P. Alivisatos, *Science*, **304**: 711 (2004).
2. A. M. Gusak, T. V. Zaporozhets, K. N. Tu, and U. Gösele, *Philos. Magazine*, **85**, No. 36: 4445 (2005).
3. H. J. Fan, U. Gösele, and M. Zacharias, *Small*, **3**, No. 10: 1660 (2007).
4. A. M. Gusak and T. V. Zaporozhets, *J. Physics: Condensed Matter*, **21**, No. 41: 415303 (2009).
5. A. M. Gusak and K. N. Tu, *Acta Mater.*, **57**, No. 11: 3367 (2009).
6. K. N. Tu, *Solder Joint Technology* (New York: Springer: 2007).
7. K. N. Tu, *Acta Metallurgica*, **21**, No. 4: 347 (1973).
8. Ya. E. Geguzin, *Diffuzionnaya Zona* [The Diffusion Zone] (Moscow: Nauka: 1979) (in Russian).
9. Ya. E. Geguzin, Y. S. Kaganovskiy, L. M. Paritskaya, and V. I. Solunskiy, *Fiz. Met. Metalloved.*, **47**, No. 4: 127 (1979) (in Russian).
10. A. M. Gusak and N. V. Storozhuk, *Phys. Met. Metallogr.*, **114**, No. 3: 197 (2013).
11. N. V. Storozhuk and A. M. Gusak, *Metallofiz. Noveishie Tekhnol.*, **35**, No. 6: 807 (2013) (in Ukrainian).
12. L. Yina and P. Borgesen, *J. Mater. Res.*, **26**, No. 3: 455 (2010).
13. G. Ross, V. Vuorinen, and M. Paulasto-Kröckel, *J. Alloys Compd.*, **677**: 127

(2016).
14. A. M. Gusak, T. V. Zaporozhets, Y. O. Lyashenko, S. V. Kornienko, M. O. Pasichnyy, and A. S. Shirinyan, *Diffusion-Controlled Solid State Reactions: in Alloys, Thin-Films, and Nanosystems* (New York: John Wiley and Sons: 2010).
15. A. M. Gusak and M. V. Yarmolenko, *J. Appl. Phys.*, **73**, No. 10: 4881 (1993).
16. A. V. Nazarov and K. P. Gurov, *Fiz. Met. Metalloved.*, **37**, No. 3: 41 (1974) (in Russian).
17. A. M. Gusak, *Metallofizika*, **14**, No. 9: 3 (1992).